Optik 125 (2014) 1875–1879

Contents lists available at ScienceDirect

Optik

journal homepage: www.elsevier.de/ijleo

Fleet algorithm for X-ray pulsar profile construction and TOA solution based on compressed sensing

Sheng-liang Li*, Kun Liu, Long-long Xiao

Institute of Space Technology, College of Aerospace Science and Engineering, National University of Defense Technology, Deya Road, Changsha, China

ARTICLE INFO

Article history:
Received 9 May 2013
Accepted 10 October 2013

Keywords:
X-ray pulsar profile
TOA
Compressed sensing
Modeling and simulation

ABSTRACT

X-ray pulse profile and time of arrival (TOA) are the two important physical quantities for pulsar navigation. With the standard and integrated X-ray pulse profiles modeled, X-ray pulse profile construction is studied and TOA is solved using compressed sensing (CS) technology. The observation matrix and waveform complete dictionary are mainly examined. A column vector-based matching pursuit algorithm is presented. The feasibility of obtaining X-ray pulse profile construction by compressed sensing technology is verified by numerical simulation. Compared with the X-ray pulse profile construction method based on epoch folding, the proposed method exhibits improved real-time performance, and its detection time for integrated X-ray pulse profile could be reduced by one order of magnitude. This proposed method can also solve for TOA solution and construct the X-ray pulse profile simultaneously, which is essential to improve pulsar navigation efficiency.

1. Introduction

Pulsar is considered a "lighthouse" owing to its stable frequency and unique location in the universe, which can help determine the position, velocity, attitude, and time for spacecraft navigation [1]. The key to X-ray pulsar navigation is the time of arrival (TOA), which can be determined by X-ray pulse profile construction. The traditional method uses epoch folding to obtain the integrated X-ray pulse profile [2,3], which is compared with the standard X-ray pulse profile for solving TOA [4–6]. The disadvantages of this technique include longer observation time and lower signal-to-noise ratio (SNR). Obviously, this method cannot meet the requirements of real time and high precision for spacecraft navigation. A signal reconstruction algorithm based on compressed sensing provides a new idea for generating an X-ray pulse profile [7–10]. This concept is first applied in X-ray pulse profile reconstruction based on compressed sensing in [7], where, however, the observation matrix does not respond to the actual process of X-ray photon detection. The author merely reconstructed the X-ray pulse profile but disregarded the solution of TOA.

In view of the above analysis, this study is organized as follows:

(1) In Section 2, the process of epoch folding is analyzed. The mathematical models of the standard X-ray pulse profile and the integrated X-ray pulse profile are established.
(2) Section 3 provides the optimization of the X-ray pulse profile model based on compressed sensing. The X-ray pulse profile waveform redundant dictionary and the observation matrix are included. The matching pursuit algorithm based on the atomic column vector is also presented.
(3) The standard X-ray pulse profile, integrated X-ray pulse profiles based on epoch folding, and X-ray pulse profile based on compressed sensing are simulated numerically in Section 4.
(4) The main conclusions are stated as follows in the last section. The proposed technique using compressed sensing generates an X-ray pulse profile more quickly compared with the traditional method. The mathematical model provides a new approach to solving the issues of real time and TOA accuracy for pulsar navigation.

2. X-ray pulse profile

An X-ray pulse profile is a curve of X-ray photon flux density detected from a pulsar with time as the variable. This profile reflects the characteristics of the pulsar. Different pulsar X-ray pulse profiles have different amplitudes and periods, among others.

2.1. Standard X-ray pulse profile mathematical model

The total number of X-ray photons detected is given by

$$I(t) = \int_0^t \lambda(\tau)d\tau + F(0) \quad (1)$$

* Corresponding author. Tel.: +86 13548658395; fax: +86 73184512301.
E-mail address: lishengliang@163.com (S.-l. Li).

0030-4026/$ – see front matter.
http://dx.doi.org/10.1016/j.ijleo.2013.10.032

where $F(0)=0$ is the number of X-ray pulsar X-ray photons at time 0. $\lambda(t)$ represents the pulsar X-ray photon flux density. Within the time $[t, s]$, the detected number of X-ray photons is described as:

$$I_t^s = \int_t^s \lambda(\tau)d\tau \tag{2}$$

$\lambda(t)$ consists of two parts, as shown below:

$$\lambda(t) = \lambda_b + \lambda_p(t) \tag{3}$$

where λ_b is a constant representing the X-ray photon background noise density. $\lambda_p(t)$, which represents the X-ray photon density, can be described as follows:

$$\lambda_p(t) = \bar{\lambda}_p \cdot u(\phi(t)) \tag{4}$$

where $\bar{\lambda}_p$ denotes the average density of pulsars. The periodic function $u(\phi(t))$ is defined as the profile function. $\phi(t)$ is the time phase, $\phi \in [0, 1)$, and $\int_0^1 u(\phi)d\phi = 1$.

$$\phi(t) = \phi_0 + \int_{t_0}^{t} fre(\tau)d\tau \tag{5}$$

where ϕ_0 is the initial phase, and $fre(t)$ represents the pulse frequency. When the rate of change of frequency and Doppler shift are squared, $fre(t)$ can be expressed as:

$$fre(t) = fre_p(t) \cdot \left(1 + \frac{v(t)}{c}\right) \tag{6}$$

where $fre_p(t)$ is the pulsar rotation frequency, and $v(t)$ is defined as the constant v. The phase function $\phi(t)$ is given by

$$\phi(t) = \phi_0 + \left[\left(1 + \frac{v(t)}{c}\right) \cdot (t - t_0) \cdot fre_p(t)\right] \tag{7}$$

Thus, the standard mathematical model of the X-ray pulse profile is expressed as:

$$\lambda(t) = \lambda_b + \bar{\lambda}_p \cdot u\left(\phi_0 + \left(1 + \frac{v(t)}{c}\right) \cdot (t - t_0) \cdot fre_p(t)\right) \tag{8}$$

When the parameters λ_b, $\bar{\lambda}_p$, ϕ_0, $u(\phi)$ are determined, the X-ray pulse profile can be constructed.

2.2. Mathematical model of the integrated X-ray pulse profile

Within the time interval δt, the probability of obtaining the number of X-ray photons, $f(i, j)$, is written as:

$$P(f(i,j), \delta t) = \frac{\left(\left(\int_{(j-1)\cdot\delta t}^{j\cdot\delta t} \lambda(t)dt\right)^{f(i,j)} \cdot \exp\left(-\int_{(j-1)\cdot\delta t}^{j\cdot\delta t} \lambda(t)dt\right)\right)}{f(i,j)!} \tag{9}$$

Within the time interval δt, the expectation and the variance of the number of X-ray photons, $f(i, j)$ are presented as follows:

$$E[f(i,j)] = var[f(i,j)] = \int_{(j-1)\cdot\delta t}^{j\cdot\delta t} \lambda(t)dt \tag{10}$$

As $\delta t \to 0$, Eq. (10) can be approximated by

$$E[f(i,j)] = var[f(i,j)] = \lambda(t_{i,j})\delta t \tag{11}$$

The pulsar X-ray density is always in the order of 10^{-5} phs$(\text{cm}^2\,\text{s})^{-1}$. To obtain a higher SNR X-ray pulse profile, the pulsar has to be observed for an extended period and pulsar X-ray photons function has to be generated by epoch folding [3,4].

Assuming t_j is the intermediate time in the jth bin, after superimposition and normalization, the detected value of the integrated X-ray pulse profile is:

$$y(t_j) = \frac{1}{N \cdot \delta t}\sum_{i}^{N} f(i,j) \tag{12}$$

During measurement of pulsar X-ray photons, the X-ray pulse profile introduces the random noise given by

$$\bar{y}(t_j) = y(t_j) + v(t_j) \tag{13}$$

where, $v(t_j)$ is the random noise with the distribution $v(t_j) \sim (0, \sigma^2)$ at time t_j.

Theoretically, when the observation time $t_f \to \infty$, the standard X-ray pulse profile $x(t)$ can be obtained. Thus, a longer time is required to obtain the X-ray pulse profile using epoch folding. The current objective is to obtain an X-ray pulse profile within a short period. After epoch folding, we determine the observations $y(t)$ for the X-ray pulse profile $x(t)$. The integrated X-ray pulse profile $x(t)$ is then reconstructed based on compressed sensing from the measured values of $y(t)$.

3. X-ray pulse profile construction based on compressed sensing

3.1. Compressed sensing

Compressed Sensing is a very efficient and fast growing signal recovery frame-work. The basic principle of CS theory is that when the image of interest is very sparse or highly compressible in some basis, relatively few well-chosen observations suffice to reconstruct the most significant nonzero components. The CS model is described as:

$$\widehat{x} = \min ||x||_0 \quad \text{s.t.} \quad y = \Phi \cdot f = \Phi \cdot \Psi \cdot x = \Theta \cdot x \tag{14}$$

where $Y \in Z^M$ is an observation vector. $f \in R^N$ is an unknown signal, which can be sparsely represented as $f = \Psi \cdot x$ in an orthonormal basis Ψ. If there are only $K(K \ll N)$ non-zero components of x, f is defined as being K-sparse. Φ denotes a $M \times N(M \ll N)$ matrix called measurement matrix. Θ is a sensing matrix compounded by Φ and Ψ.

In order to successfully reconstruct a signal with incomplete measurements, Θ must satisfy a special property called the restricted isometry property (RIP); that is, for all K-sparse $x \in R^N$, a constant $\delta_k \in (0, 1)$ exists so that

$$1 - \delta_k \le \frac{||\Theta x||_2^2}{||x||_2^2} \le 1 + \delta_k \tag{15}$$

There are many optimal methods to solve the problem described in Eq. (14), such as basis pursuit (BP), matching pursuit (MP), iterative thresholding, and total variation (TV) specially for signal reconstruction.

From the above model, we can see that CS contains three critical parts: signal sparsity, random observation and recovery algorithm.

3.2. Pulse signal observation

Assuming that the standard X-ray pulse profile is $p(n)$ and the integrated X-ray pulse profile is $x(n)$, the value of the observed X-ray pulse profile is $y(m)$, for $n = 1, 2, \ldots, N$ and $m = 1, 2, \ldots, M, M \le N$.

Pulsar detection can be considered as random sampling from discrete integrated X-ray pulse profile $x(n)$. After detection in several periods, the observation vector $y(m)$ can be obtained by epoch folding.

$$y(m) = \Phi \cdot x(n) \tag{16}$$

where Φ denotes a $M \times N(M \ll N)$ matrix called measurement matrix. $\varphi_{m\times n}$ is the elements of the measurement matrix Φ. After epoch folding, the arrival times of pulsar X-ray photons are concentrated in the first phase period $\phi \in [0, 1)$. Each phase period is divided into N bins. Assuming $y(m)$ is at the time $t_{m,n}$ when $\varphi_{m\times n} = 1$, and the remaining elements of the line are all zero, the measurement matrix Φ is known as an ill-conditioned matrix.

3.3. Pulse signal sparsity

The relationship between the standard X-ray pulse profile and the integrated X-ray pulse profile can be expressed as follows:

$$x(t) = b + a \cdot p(t - \tau) + n(t) \tag{17}$$

where τ is the time delay, TOA is the time delay known as $TOA = n\tau$. a is the amplitude factor, and $n(t)$ is the random noise. b is the background noise, a constant which can be corrected during normalization.

According to the above formula, the integrated X-ray pulse profile can be viewed as a period and amplitude normalization and transformation from the standard X-ray pulse profile. Thus, we design the complete dictionary of integrated X-ray pulse profile as:

$$\Psi := \{\varphi_n(t) | \varphi_n(t) = p(t - n\tau)\}, \quad n \in \{1, 2, \ldots, N\} \tag{18}$$

The integrated X-ray pulse profile $x(t)$ can be projected on the complete dictionary, described below.

$$x(t) = \sum_{i=1}^{K} a_i \varphi_i(t) \tag{19}$$

where $x(t)$ is a one-order sparse signal for $K = 1$.

3.4. Pulse profile recovery algorithm

On the basis of the sparse representation of the X-ray pulse profile, the observation model can be expressed as:

$$y(m) = \Phi_{m\times n} \cdot x(n) = \Phi_{m\times n} \cdot \Psi_{n\times n} \cdot a = \Theta_{m\times n} \cdot a_n \tag{20}$$

where $\Theta_{m\times n}$ is a typical ill-conditioned matrix. Thus, the problem is transformed into a compressed-sensing-based optimization model for solving

$$\arg\min_a ||a_n||_1 \quad \text{s.t.} \quad y = \Phi\Psi a_n = \Theta a_n \tag{21}$$

Because the integrated X-ray pulse profile can be considered the product of some column vectors in a complete dictionary and the amplitude. In this paper, we propose a column vector-based matching pursuit algorithm to determine TOA while solving for the X-ray pulse profile.

The cost function of the column vector-based matching pursuit algorithm is:

$$\min \sum ||y - \Theta_{m\times n} a_n|| \tag{22}$$

The specific steps of the algorithm are as follows:

Step (1) Initialization. The initial value of the sparse vector is $a_1^0 = 0$, and the residuals are initialized as $r_0^0 = r_1^0 = ||y||_2$. The sets of selected atomic column vectors are initialized to E_0^0 and E_1^0, which are empty sets. The column circular pointer is set to $n = 1, n \in [1, N]$. The sparse vector pointer is set to $k = 1, k \in [1, (a_{\max} - a_{\min}/\delta a)]$.

Step (2) Selection of the nth column atomic vector.

Step (3) Selection of the kth sparse vector a_n^k corresponding to the nth column atomic vector and solution of the residuals $r_n^k = ||y - \Theta_{m\times n} a_n^k||_2$.

Step (4) Updating the set of residuals and the selected atomic column vectors $r_n^k = \min\{r_n^{k-1}, r_n^k\}$. The serial number set of the selected atomic column vector is $E_n^k = E_n^{k-1} \cup n_k$.

Step (5) Iteration. $a_n^k = a_n^k + \delta a$, where δa is the step length. The circular pointer is $k = k + 1$. The iteration will stop when the termination condition is satisfied; otherwise, the operation returns to (3).

Step (6) Updating the set of residuals and the selected atomic column vector $r_n^k = \min\{r_{n-1}^k, r_{\bar{n}}^k\}$. The serial number set for the chosen atomic column vector is $E_n^k = E_{n-1}^k \cup n_{\bar{k}}$.

Step (7) Iteration. The circular pointer is $n = n + 1$. The iteration will stop when the termination condition is satisfied; otherwise, the operation returns to (2).

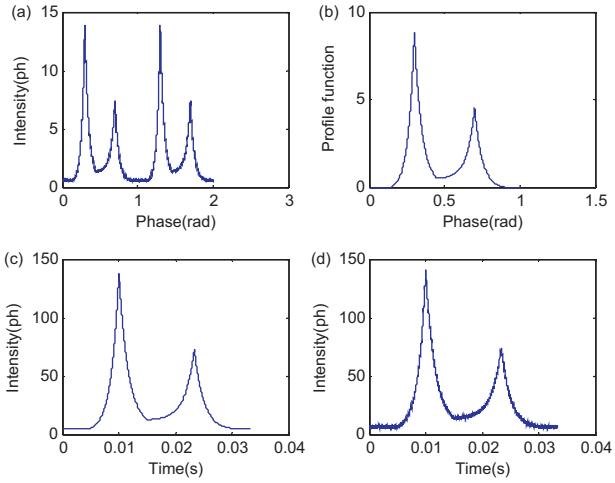

Fig. 1. Standard X-ray pulsar profile: (a) X-ray pulsar profile of Crab; (b) profile function; (c) X-ray pulsar profile; (d) X-ray pulsar profile with noise.

4. Simulations

To verify the feasibility and efficiency of the algorithm for the X-ray pulse profile construction and solving for TOA based on compressed sensing, the standard X-ray pulse profile, integrated X-ray pulse profile based on epoch folding, and integrated X-ray pulse profile based on compressed sensing are simulated. The two integrated algorithms are compared in terms of their advantages and disadvantages.

4.1. Simulation of the standard X-ray pulse profile

The Crab X-ray pulse profile is presented as an example in Fig. 1(a). As the shape of Crab X-ray pulse profile is similar to the shape of exponential function, the profile function is simulated by the exponential function.

$$u(\phi) = a \cdot e^{k\phi} + c \tag{23}$$

where $\int_0^1 u(\phi)d\phi = 1$. Considering the characteristic of the Crab profile function, we can obtain a Crab profile function using MATLAB, as shown in Fig. 1(b).

In accordance with the profile function, the pulsar density function can be simulated. Assuming that the pulse period is the constant $P = 0.0334$ s, initial time $t_0 = 0$, and the relative speed

between the detector and the pulsar in direction of the pulsar vector is the constant $v(t) = v = 3\,\text{km/s}$, $\lambda_b = 5\,\text{ph/(cm}^2\,\text{s)}^{-1}$, $\bar{\lambda}_p = 15\,\text{ph/(cm}^2\,\text{s)}^{-1}$ when the phase of the pulse peak is $\phi_0 = 0.3$. The X-ray pulse profile with noise is shown in Fig. 1(c).

4.2. Simulation of the integrated X-ray pulse profile

The integrated X-ray pulse profile can be obtained using non-homogeneous Poisson random targeting experiments. First, according to the non-homogeneous Poisson distribution, the arrival times of pulsar X-ray photons are generated. Assuming that the arrival time of the kth X-ray photon is t_k, $\delta t = X$, and $F_{x|t_k=t}(x|t_k = t)$ is the distribution of $X = t_{k+1} - t_k$,

$$P(X \geq x|t_k = t) = 1 - F_{x|t_k=t}(x|t_k = t) \tag{24}$$

From Eq. (24) and $P(X \geq x|t_k = t)$, the probability of detecting 0 X-ray photon in δt is

$$P(X \geq x|t_k = t) = P(0, \delta t) = \exp\left(-\int_t^{t+x} \lambda(t)dt\right) \tag{25}$$

Thus, the distribution of $X = t_{k+1} - t_k$ can be expressed as:

$$F_{x|t_k=t}(x|t_k = t) = 1 - \exp\left(-\int_t^{t+x} \lambda(t)dt\right) \tag{26}$$

with $y = F_{x|t_k=t}(x|t_k = t)$ as the inverse function of $y(x)$, $y^{-1}(x) = X$ is expressed as follows:

$$y = 1 - \exp\left(-\int_t^{t+x} \lambda(\tau)d\tau\right) \tag{27}$$

The above equation can be rewritten as:

$$y = 1 - \exp\left(-\left(\int_0^{t+x} \lambda(\tau)d\tau - \int_0^{t} \lambda(\tau)d\tau\right)\right) \tag{28}$$

If $\varphi(t) = \int_0^t \lambda(\tau)d\tau$, then Eq. (29) can be expressed as:

$$y = 1 - \exp(\varphi(t) - \varphi(t + x)) \tag{29}$$

The inverse solution for x is

$$x = -t + \varphi^{-1}[\varphi(t) - \ln(1 - y)] \tag{30}$$

$y \in (0, 1)$, $(1 - y) \in (0, 1)$. Thus,

$$X = -t + \varphi^{-1}[\varphi(t) - \ln(y)] \tag{31}$$

Considering $\delta t = X = t_{k+1} - t_k$,

$$t_{k+1} = \varphi^{-1}[\varphi(t_k) - \ln(y)] \tag{32}$$

where $\varphi(t) = \int_0^t \lambda(\tau)d\tau$ as $\delta t \to 0$. The above equation can be approximated as follows:

$$t_{k+1} = t_k + \frac{-\ln(y)}{\lambda(t_k)} \tag{33}$$

The steps of epoch folding simulation are presented as follows:

Step (1) Within the interval (0,1), generate a random variable y, $t_0 = 0$ is used as the initial time.
Step (2) Calculate the next arrival time of the X-ray photons using Eq. (33).
Step (3) Compare t_k with the detection time t_f, if $t_k \leq t_f$, return to step (1), otherwise, exit.
Step (4) Store the arrival times of all X-ray photons. Calculate the flux density at the TOA, and obtain the X-ray pulse profile using epoch folding.

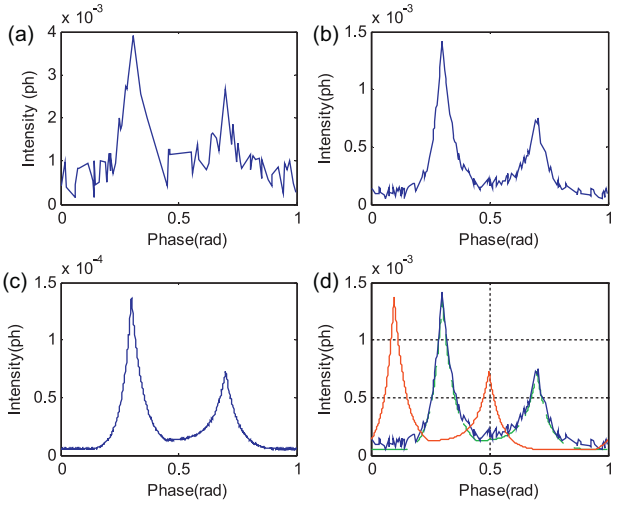

Fig. 2. X-ray pulsar profile: (a) measurement time 3.34 s; (b) measurement time 33.4 s; (c) measurement time 334 s; (d) X-ray pulsar profile construction based on compressed sensing (the real line is the standard X-ray pulsar profile, the broken line is the pulsar profile based on CS). (For interpretation of the references to color in this text, the reader is referred to the web version of the article.)

X-ray pulse profile construction based on compressed sensing is investigated using the following simulation steps:

Step (1) Using the Gaussian random shooting experiment, generate a set of pulsar X-ray photon arrival times and record the number of X-ray photons at each time.
Step (2) Obtain the integrated X-ray pulse profile observed vector $y[m]$ by epoch folding, and record the observation matrix. The compressed sensing optimization model of the integrated X-ray pulse profile is established.
Step (3) Obtain the sparse vector a_n by the column vector-based matching pursuit algorithm and calculate TOA $= d = n\tau$, recovery integrated X-ray pulse profile $x(n) = \Psi_{n\times n} \cdot a_n$.

The simulation parameters are set similar to Section 4.1. Fig. 2a–c shows the integrated X-ray pulse profile at the observation times $t_f = 3.34$ s, $t_f = 33.4$ s, and $t_f = 334$ s. For the observation time $t_f = 33.4$ s, compare the integrated X-ray pulse profile based on epoch folding. The integrated X-ray pulse profile based on compressing sensing and the standard X-ray pulse profile are shown in Fig. 2d. The pulse arrival time is calculated as TOA $=$ 0.0267 s.

As shown in Fig. 2, when the detection time $t_f = 3.34$ s, the X-ray pulse profile amplitude fluctuates frequently. At $t_f = 334$ s, the detection X-ray pulse profile resembles the standard X-ray pulse profile. Therefore, as the observation time increases, the integrated X-ray pulse profile based on epoch folding becomes more similar to the standard X-ray pulse profile. As indicated in Fig. 2d, the detection time $t_f = 33.4$ s, the X-ray pulse profile amplitude fluctuates frequently by epoch folding, and the TOA has a larger error, which is not propitious to TOA solution. The X-ray pulse profile construction based on compressed sensing can obtain a higher SNR X-ray pulse profile as well as a high-precision TOA.

5. Conclusions and discussion

In this paper, the mathematical models of the standard X-ray pulse profile and the cumulative X-ray pulse profile are established. Integrated X-ray pulse profile construction based on epoch folding exhibits a poor real-time feature. The X-ray pulse profile

construction and TOA solving based on compressed sensing is presented. The observation matrix and waveform complete dictionary are investigated. The optimization models based on compressed sensing is constructed, and a column vector-based matching pursuit algorithm is presented. In accordance with the numerical simulation, we obtain a high-precision X-ray pulse profile and TOA using few periods. We analyzed the impact of detection time in X-ray pulse profile establishment and concluded that the time of the X-ray pulse profile construction based on compressed sensing is less than that based on epoch folding by one order of magnitude. From the results, we established the significance of X-ray pulsar profile construction and TOA solution based on compressed sensing in improving the real-time performance and precision of TOA in pulsar navigation.

Acknowledgment

This work was supported by the National Natural Science Foundation of China (Grant no. 61271440).

References

[1] S.I. Sheikh, D.J. Pines, P.S. Ray, K.S. Wood, M.N. Lovellette, Spacecraft navigation using X-ray pulsars, J. Guid. Control Dyn. 29 (2006) 49–63.
[2] L.I. Jian-xun, K.E. Xi-zheng, The maximum-likelihood estimate of TOA accuracy for X-ray pulsar signal based on Poisson process, Acta Astron. Sin. 51 (3) (2010) 263–270 (in Chinese).
[3] H.J. Hu, B.S. Zhao, L.Z. Sheng, X.F. Sai, Q.R. Yan, B.M. Chen, P. Wang, X-ray photon counting detector for X-ray pulsar-based navigation, Acta Phys. Sin. 61 (1) (2012) 019701–19705 (in Chinese).
[4] A.A. Emadzadeh, J.L. Speyer, X-ray pulsar-based relative navigation using epoch folding, IEEE Trans. Aerospace Electron. Syst. 47 (4) (2011) 2317–2328.
[5] A.A. Emadzadeh, J.L. Speyer, On modeling and pulse phase estimation of X-ray pulsars, IEEE Trans. Signal Process. 58 (9) (2010) 4484–4495.
[6] A.A. Emadzadeh, J.L. Speyer, Relative navigation between two spacecraft using X-ray pulsars, IEEE Trans. Control Syst. Technol. 19 (5) (2011) 1021–1035.
[7] Z. Su, L.P. Xu, W. Gan, Pulsar profile construction algorithm based on compressed sensing, Sci. Sin. Phys. Mech. Astron. 41 (05) (2011) 681–684 (in Chinese).
[8] L.L. Xiao, K. Liu, D.P. Han, J.Y. Liu, A compressed sensing approach for enhancing infrared imaging resolution, Opt. Laser Technol. 44 (2012) 2354–2360.
[9] L.L. Xiao, K. Liu, D.P. Han, CMOS low data rate imaging method based on compressed sensing, Opt. Laser Technol. 44 (2012) 1338–1345.
[10] D.L. Donoho, Compressed sensing, IEEE Trans. Inform. Theor. 52 (4) (2006) 1289–1306.